Active microwave device applications of ferroelectric thin films

D.B. Chrisey, J.S. Horwitz, J.M. Pond, R.C.Y. Auyeung, P.C. Dorsey, S.B. Qadri, and L.A. Knauss

Naval Research Laboratory, Washington, D.C.

C.H. Mueller and R.M. Yandrofski

Superconducting Core Technologies, Golden, CO

ABSTRACT

We describe the deposition of $Sr_xBa_{1-x}TiO_3$ ($0.2 \leq x \leq 0.8$) thin films by pulsed laser deposition and the issues related to their application as active microwave device components. The $Sr_xBa_{1-x}TiO_3$ thin films (~5000 Å) deposited at 775-850 °C in 350 mTorr of oxygen onto (100) MgO and $LaAlO_3$ were smooth, single phase, and epitaxial with the underlying substrate. Highly oriented $Sr_{0.5}Ba_{0.5}TiO$ films on $LaAlO_3$ with x-ray rocking curves of 72 arc seconds were observed. The dielectric constant of $Sr_{0.5}Ba_{0.5}TiO_3$ thin films, determined from the signal in patterned transmission lines between 100 kHz and 0.1 GHz, was ~20% of that observed for the bulk and the zero field temperature dependence was broad in comparison to the sharply peaked behavior seen in bulk. The dielectric loss tangent was measured as a function of stoichiometry for $Sr_xBa_{1-x}TiO_3$ ($0.2 \leq x \leq 0.8$) thin films (3-5 μm) at room temperature and at 9.2 GHz. Loss tangent values were found to be highly sensitive to the Curie temperature of the film. Loss tangent values as low as 0.1% were obtained for $Sr_{0.8}Ba_{0.2}TiO_3$. The results for $Sr_xBa_{1-x}TiO_3$ thin films presented in this paper are encouraging for future applications in active microwave devices.

1. INTRODUCTION TO PULSED LASER DEPOSITION

Many important next generation Naval and commercial systems will depend on thin films of complex materials to achieve improved performance in terms of size, input power, and system lifetime. The applications for thin films of these materials ranges from electronics (e.g., high T_c superconductors, ferroelectrics, ferrites, and dielectrics) to degradation-resistant coatings on structural materials (e.g., tribological and wear-resistant ceramic coatings). Thin films of these next generation materials are technologically important because they exhibit improved physical and electrical properties. Unfortunately, the most desired of these materials are typically multicomponent and have a complex crystalline structure. Furthermore, their electrical properties are often highly anisotropic which adds the additional requirement of oriented or epitaxial thin film growth. Because of the strong market demand for improved system performance there exists considerable interest in the Navy and elsewhere to develop better ways to deposit and process thin films of these complex materials.

Pulsed laser deposition (PLD) has repeatedly demonstrated itself as the superior physical vapor deposition technique for the production of high quality thin films and multilayers of complex, multicomponent materials such as the high T_c superconductors (e.g., $YBa_2Cu_3O_7$). For a comprehensive review of PLD see ref. 1. Stoichiometric, epitaxial, and phase pure thin films of these materials cannot be *easily* deposited by other more conventional physical vapor deposition techniques such as e-beam co-evaporation or sputtering. There would be little argument that PLD was rediscovered and popularized in the late 1980's to meet the demanding challenges of processing high quality thin films of the high T_c superconductors. PLD quickly gained wide acceptance as a novel physical vapor deposition technique because of the high quality and reproducibility of the resulting

0-8194-1750-5/95/$6.00

high T_c superconducting thin films. Shortly thereafter, the generic advantages of PLD for the deposition of thin films of complex multicomponent materials were recognized and applied to ferroelectrics, ferrites and even biocompatible ceramics with similar success.[1]

The principal advantages of PLD for the deposition of thin films of multicomponent ceramics is the ability to transfer target stoichiometry to the growing film, the simplicity of the experimental set-up (see Fig. 1), and the ability to deposit films in a high pressure reactive ambient (~0.1 Torr), i.e., the latter gives you the ability to tailor the oxygen doping in oxide films. In simple terms, the stoichiometric transfer occurs because the pulsed excimer laser rapidly flash-evaporates the ceramic target pellet. Unlike the other continuous beam techniques (e.g., sputtering and e-beam co-evaporation), energy is delivered to the target source only during the laser pulse and most of the material deposition on the substrate takes less than 1 ms. This yields instantaneous deposition rates on the order of 10^4 to 10^5 Å/sec which is at least three to four orders of magnitude larger than other techniques. Details of the material deposition and film self-assembly are not well understood and are especially hard to model due, in part, to the multicomponent and varied nature of the ejecta, i.e., neutral and ionized atoms, oxides, and small clusters with a wide variety of kinetic energies are incident on the substrate.

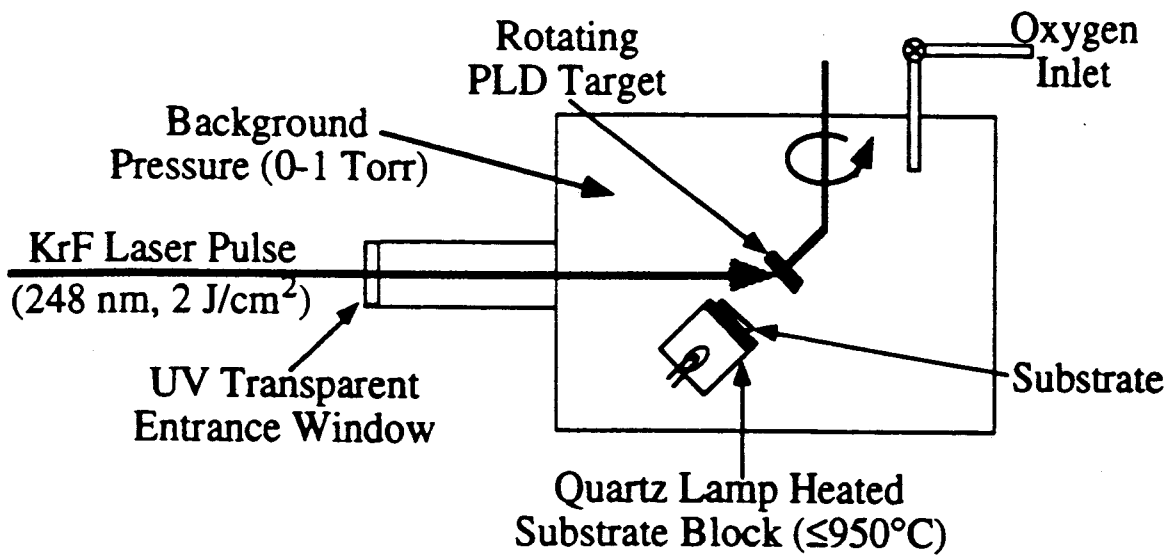

Figure 1. Schematic diagram of the pulsed laser deposition chamber used. The target-substrate distance is fixed at ~3 cm.

2. INTRODUCTION TO HTS MICROWAVE DEVICES

The advantages of HTS thin films for electronics applications were first realized in simple passive microwave devices such as resonators, filters, and short delay lines. Patterned HTS films offered orders of magnitude lower conductor losses due to the extremely small microwave surface resistance, R_s, intrinsic to superconductors. The microwave surface resistance is a useful figure-of-merit for microwave devices as it is proportional to the quality factor, Q, of resonant structures and inversely proportional to the insertion loss in transmission structures. In many situations, (e.g., bandpass filters in communication satellites) the lower conductor losses improves the device performance and reduces the weight enough to justify the added burden of the required cryogenic cooling.

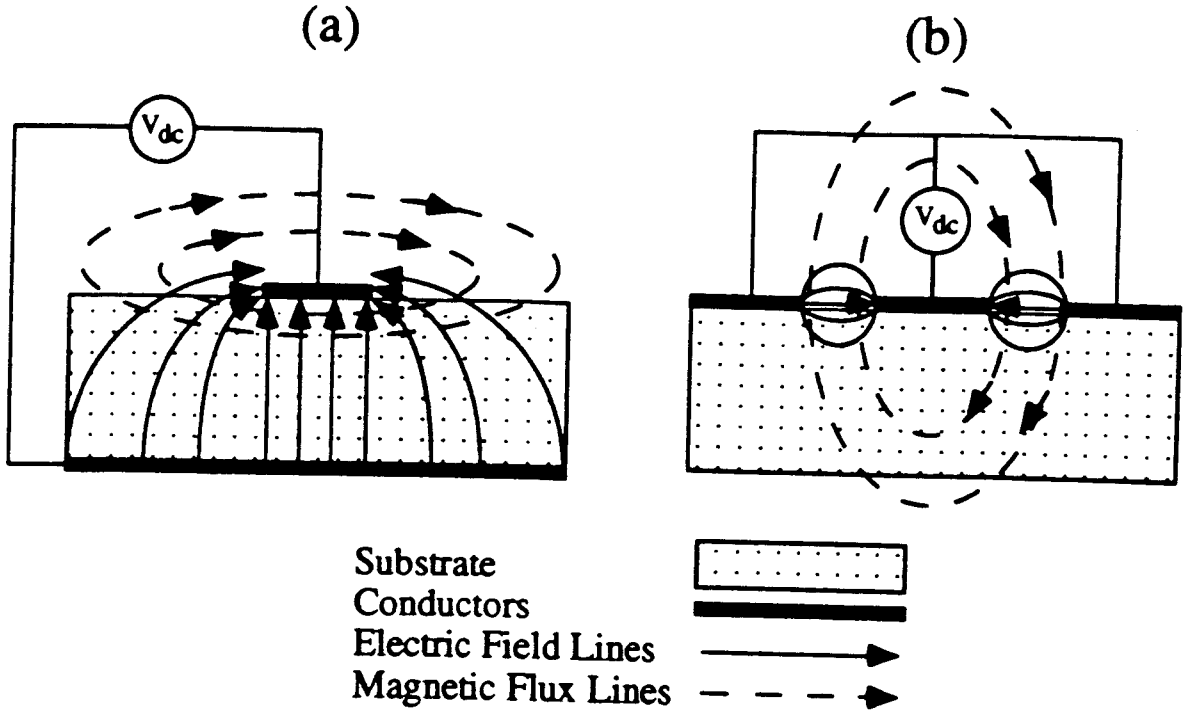

Figure 2. Cross sections of two different circuit implementations for thin film HTS microwave circuits. On the left (a) is the microstrip implementation and the right (b) is the coplanar implementation. The microwave signal travels into the page. Typically, dielectric substrates are 0.1 cm thick and patterned HTS lines are ~0.1 cm wide.

Passive microwave circuits made from HTS thin films have typically been implemented in one of either two forms, microstripline or coplanar wave guide as shown in Fig. 2. In the microstrip implementation the electromagnetic waves travel almost exclusively in the dielectric between the top and bottom conductors. For the early passive HTS microwave devices, the dielectric was simply the substrate used to grow the thin film as shown in Fig. 2a).[2] Subsequently, multilayers of HTS and dielectrics were fabricated and used in device fabrication or to analyze superconducting properties.[3] It was at this stage that many researchers realized the novel circuit functions that could be gained by replacing the conventional dielectric with a ferroelectric thin film and that pulsed laser deposition could be used to deposit both materials.[4] More will be said about the relative merits of the circuit implementations of Fig. 2 once the active dielectric property of ferroelectrics has been introduced. The last type of microwave circuit implementation, called stripline, requires five thin film layers as well as an added planarization step and it has not been demonstrated as yet for HTS microwave circuits.

3. INTRODUCTION TO FERROELECTRICS

Ferroelectrics have a wealth of interesting and useful properties because of their noncentrosymmetric crystal lattice structure, which results in spontaneous polarization. Device application areas for ferroelectric thin films include high-dielectric constant trench capacitors for high density dynamic random access memories (DRAMS), nonvolatile random access memories (NVRAMS), piezoelectric transducers for microelectrical mechanical systems (MEMS), pyrolytic detectors, optical displays, and linear and nonlinear

electrooptic applications. The ferroelectric property of interest in this paper is called the "active dielectric" property. In a ferroelectric, the dielectric constant can be varied by applying an electric field. The variable dielectric can be used in a microwave device to change the phase velocity allowing the device characteristics to be tuned in real time for a particular application.

The use of ferroelectric materials as a non-linear dielectric at microwave frequencies and the integration of tunable dielectrics with conductors that have low R_s is actively being investigated for a variety of advanced high frequency applications.[5] Thin films (1-10 μm) offer a unique advantage over bulk materials for these applications. Large electric fields (0-200 kV/cm) can be achieved in thin films using low bias voltages (0-10 V). All passive microwave devices based on signal transmission and resonance, including delay lines, oscillators, and filters can now be made active by using a ferroelectric thin film as the variable dielectric, because with the application of an electric field, the phase velocity in the device can be continuously varied. Furthermore, unlike active ferrite devices where the biasing magnetic field must be changed by changing a current through a wire loop, in active ferroelectric devices a voltage is changed. This yields a device response time which is orders of magnitude faster. This and the small control voltages are the two principal advantages of active microwave devices based on ferroelectric thin films. Although the active dielectric property of bulk ferroelectrics has been known for decades, it has only been through the recent use of PLD that this property could be exploited in thin film devices. To make this technology work requires high quality ferroelectric thin films. PLD has been used extensively to deposit epitaxial thin films of a number of perovskite ferroelectrics including $Pb(Zr,Ti)O_3$, $(Sr,Ba)NbO_3$, $PbGe_3O_5$, and $(Sr,Ba)TiO_3$ and has helped to meet the needs of many of the aforementioned applications.[1]

Table I. Crystalline structure and bulk lattice constants for $YBa_2Cu_3O_7$, $SrTiO_3$, $BaTiO_3$, and two common substrate materials.

Material	Structure	a(Å)	b(Å)	c(Å)
$YBa_2Cu_3O_7$	Orthorhombic	3.856	3.870	11.666
$SrTiO_3$	Cubic	3.905	-	-
$BaTiO_3$	Tetragonal	4.003	4.022	-
$Sr_{0.5}Ba_{0.5}TiO_3$	Cubic	3.947	-	-
$LaAlO_3$	Rhombohedral	3.787	-	-
MgO	Cubic	4.210	-	-

The ferroelectric $Sr_xBa_{1-x}TiO_3$ was used for active dielectric applications in our work because it has demonstrated a relatively low loss in the bulk state and because its Curie temperature (the temperature defining the boundary between the ferroelectric and paraelectric phases) can be continuously varied between 30 and 400 K as the Ba doping (1-x) is varied between 0 and 1, respectively. The ability to position the Curie temperature is important as the dielectric constant and the dielectric tunability are maximized at this temperature. Depending on the application, the Curie temperature can be positioned relative to the devices operating temperature. With PLD, this full range of doping can be easily and reproducibly achieved through the use of targets with correspondingly different stoichiometries. In addition, $Sr_xBa_{1-x}TiO_3$ offers the potential to utilize $YBa_2Cu_3O_7$ as the

metallization layer(s) because their close lattice match allows them to be grown heteroepitaxially. In Table I we give the crystal structure and the lattice constants for $YBa_2Cu_3O_7$, $BaTiO_3$, $SrTiO_3$, as well as the common dielectric substrates $LaAlO_3$ and MgO.

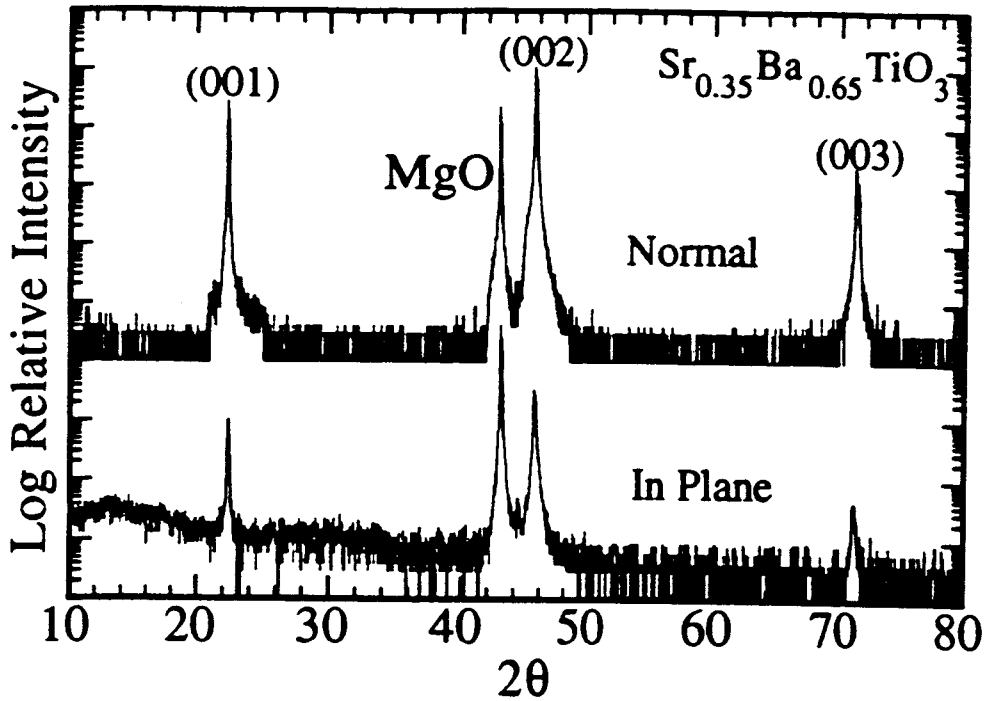

Figure 3. X-ray diffraction from an $Sr_xBa_{1-x}TiO_3$ (x=0.35) thin film deposited onto (100) MgO for both normal and in plane alignment.

It is important to understand the advantages and disadvantages of the two different circuit implementations in Fig. 2 for active dielectric applications because there are trade-offs in terms of materials processing and electrical performance which must be balanced. For example, in the coplanar wave guide practical devices can be made using either normal metal or superconducting metallization. Normal metals expand the devices operating temperature above 77 K to room temperature and beyond. In this circuit approach, a ferroelectric film will be added as either an overlay to what is shown in Fig. 2 or underneath as the first deposited layer. Since the electric fields are not confined to the ferroelectric layer, the coplanar wave guide approach offers ~50% less tunability and makes it more difficult to model the dielectric properties of the ferroelectric from measured microwave performance. Similarly, it is harder to pre-design the circuit for specific performance. Furthermore, the gaps between the center conductor and those to either side are ≥ 10 μm making the applied electric field less effective in changing the dielectric constant. The principal advantage of the coplanar wave guide approach is that only one or two (depending on if HTS metallization is used) high quality thin films have to be deposited. In the microstrip approach, the bottom ground plane is deposited on a dielectric substrate. On top of the ground plane is deposited the ferroelectric layer and then the patterned transmission line, i.e., three layers must be deposited and the latter two must be patterned. While this approach offers larger tunability because the fields are confined to the

ferroelectric layer and it is much easier to analyze the ferroelectric properties from device performance, for practical 50 Ω impedance-matched devices it requires thick ferroelectric layers (~50 μm).

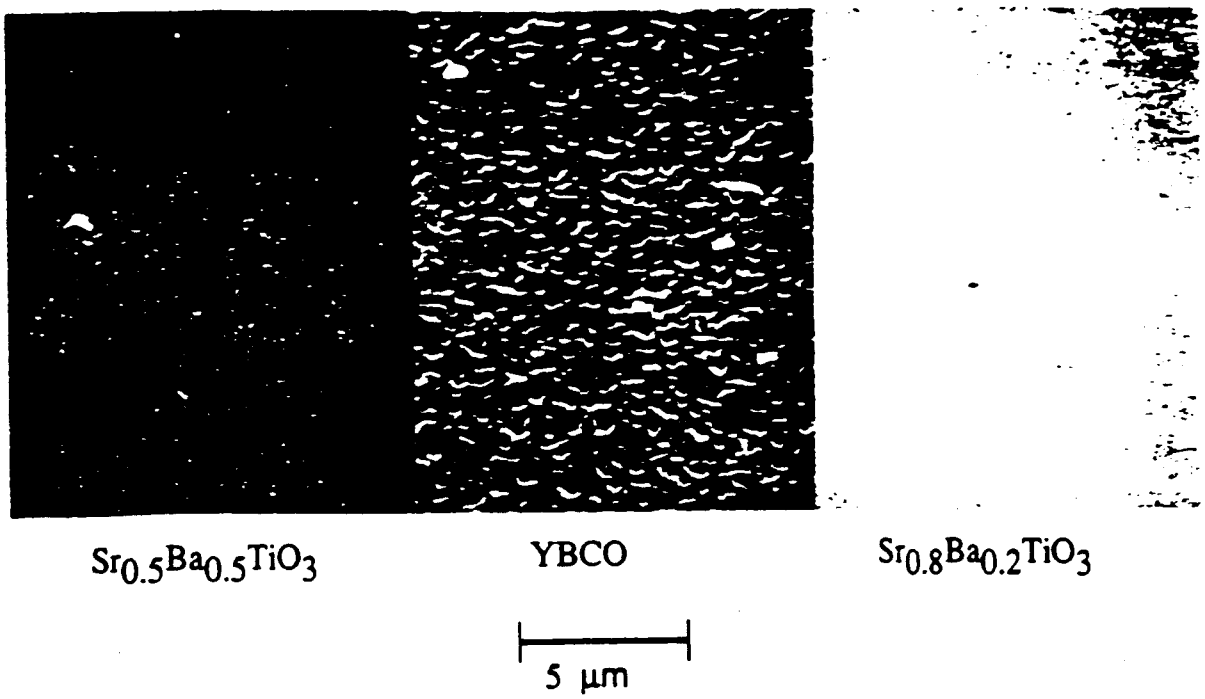

Figure 4 A scanning electron micrograph of a $Sr_{0.5}Ba_{0.5}TiO_3$ thin film , a $YBa_2Cu_3O_7$ thin film, and a $Sr_{0.8}Ba_{0.2}TiO_3$ thin film at the same magnification. The 5 μm length bar is the same for all micrographs. The intrinsically smooth surface morphology of pulsed laser deposited $Sr_xBa_{1-x}TiO_3$ thin films is apparent.

This paper describes the growth of epitaxial $Sr_xBa_{1-x}TiO_3$ thin films by pulsed laser deposition. The $Sr_xBa_{1-x}TiO_3$ films were deposited onto dielectric substrates and onto $YBa_2Cu_3O_7$-coated substrates. Post-deposition characterization included x-ray diffraction, Rutherford backscattering, and scanning electron microscopy. In addition, the films were also characterized for active microwave device applications by measuring the dielectric constant as a function of field and temperature and the loss tangent as a function of Sr to Ba doping.

4. EXPERIMENTAL ARRANGEMENT

$Sr_xBa_{1-x}TiO_3$ ($0.2 \leq x \leq 0.8$) and $YBa_2Cu_3O_7$ thin films and multilayers were grown by pulsed laser deposition on dielectric substrates ((100) MgO and $LaAlO_3$). The output of a short pulsed excimer laser (5-10 Hz, 248 nm, 30 nsec FWHM) was focused onto a rotating stoichiometric target pellet at 45° to an energy density of ~2 J/cm^2. The ablation took place in a turbopumped chamber maintained at a dynamic (~10 sccm) equilibrium pressure of 350 mTorr of oxygen. The ablated material was collected on a substrate ~3 cm away from the target and coaxial with the targets surface normal. The 1 cm^2 substrates were attached with silver paint to a stainless steel block heated with two 360 watt quartz halogen bulbs. A schematic diagram of this experimental set-up is shown in Fig. 1. X-ray diffraction patterns were obtained using Cu K_α radiation from a rotating anode source using the standard θ-2θ geometry.

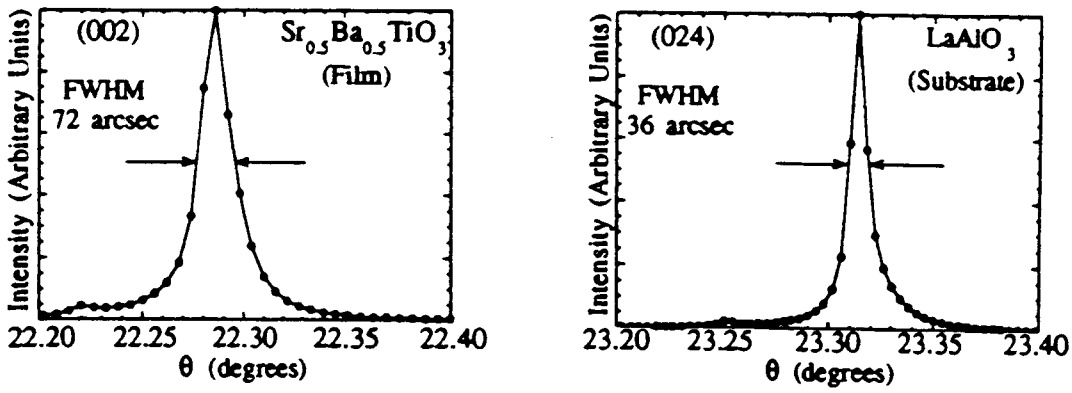

Figure 5. X-ray rocking curves for the $Sr_{0.5}Ba_{0.5}TiO_3$ film (002) and the LaAlO3 substrate (024) reflection measured using a high resolution four circle diffractometer with synchrotron radiation (8.0 keV) on the NRL beam line at the National Synchrotron Light Source at Brookhaven National Laboratory. These data indicate the high crystalline quality of PLD ferroelectric thin films.

High frequency characterization was made on both patterned and unpatterned $Sr_xBa_{1-x}TiO_3$ films and on $Ag/Sr_xBa_{1-x}TiO_3/YBa_2Cu_3O_7$ multilayers. On the $Ag/Sr_xBa_{1-x}TiO_3/YBa_2Cu_3O_7$ trilayers the Ag layer was photolithiographically patterned into 10.8 μm wide by 1 cm long transmission lines. The transmitted signal (S_{21}) was then analyzed on an HP 8753 network analyzer from 100 kHz to 0.1 GHz to determine the dielectric constant and it's field dependence. Loss tangent measurements were made on unpatterned films using a cavity perturbation technique at 9.2 GHz. In this technique, a $Sr_xBa_{1-x}TiO_3$ film is placed in a copper cavity and the change in cavity resonance is analyzed. The change in the center frequency and the cavity Q were used to determine the real and imaginary parts of the dielectric susceptibility.

5. THIN FILM FERROELECTRIC RESULTS AND DISCUSSION

Previously, it was shown that the crystalline quality of $Sr_xBa_{1-x}TiO_3$ ($0.2 \leq x \leq 0.8$) thin films on (100) MgO, as a function of substrate temperature, was optimized at ~850°C, which was the highest temperature attempted.[6] At this temperature the deposited $Sr_xBa_{1-x}TiO_3$ thin films were single phase, (100) oriented, and had narrow x-ray rocking curve widths (FWHM of Γ(100) ~0.7°). As shown in Fig. 3, an $Sr_xBa_{1-x}TiO_3$ film (x=0.35) deposited on (100) MgO is single phase and epitaxial as shown by both the normal and in plane diffraction. In Fig. 3, only the (100) reflections are observed.

The x-ray diffraction pattern of the crystal structure for $Sr_xBa_{1-x}TiO_3$ thin films was extremely sensitive to the particular substrate used. For $Sr_xBa_{1-x}TiO_3$ films deposited onto $LaAlO_3$ substrates single phase and oriented films were achieved at temperatures ~50-75°C lower than for MgO. The x-ray rocking curve widths for $Sr_xBa_{1-x}TiO_3$ thin films on $LaAlO_3$ were extraordinarily narrow, i.e., at the 1/6° resolution of the diffractometer. Further structural characterization of the film was made using monochromatic synchrotron

radiation (8.0 keV) from the National Synchrotron Light Source at the Brookhaven National Laboratory using the X-14B beam line. Fig. 4 shows the rocking curve for the $Sr_xBa_{1-x}TiO_3$ (x=0.5) thin film (002) reflection and the $LaAlO_3$ (024) reflection from the substrate. The FWHM for $Sr_xBa_{1-x}TiO_3$ (x=0.5) was found to be 72 arc seconds and the substrate to be 36 arc seconds.[7] Although there is a large lattice mismatch between the $Sr_xBa_{1-x}TiO_3$ film and the $LaAlO_3$ substrate of ~4% (see Table I), the rocking curve width is comparable or better than that seen for semiconducting films grown by molecular beam epitaxy for similar conditions of lattice mismatch and thicknesses.

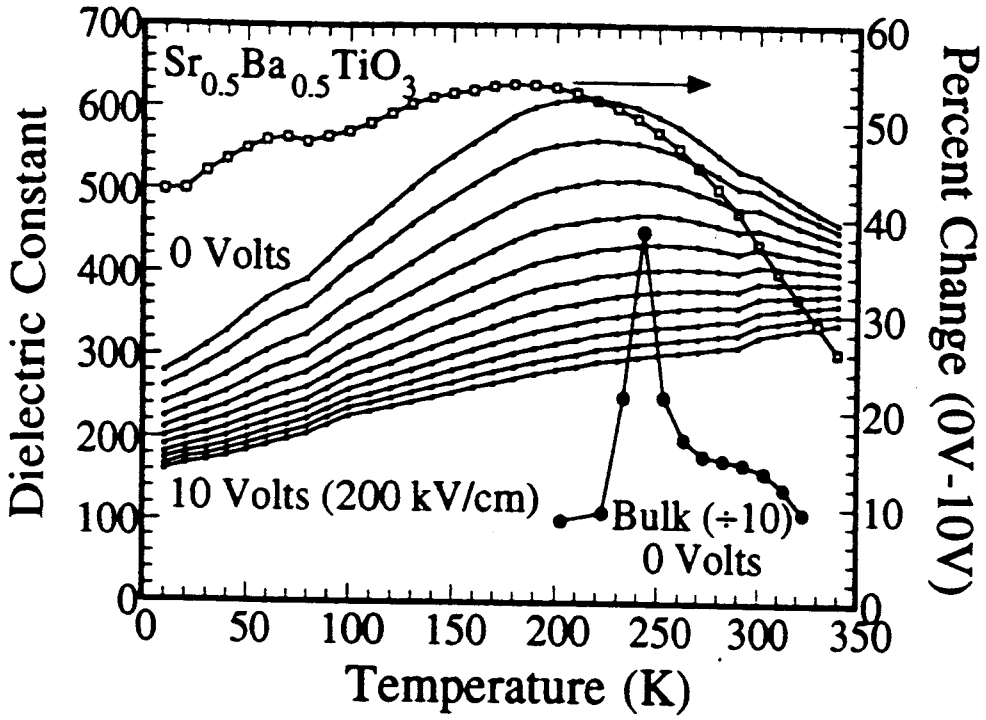

Figure 6. The dielelectric constant for an $Sr_{0.5}Ba_{0.5}TiO_3$ thin film versus temperature for several applied voltages. These data illustrate the active dielectric property on which the new microwave devices will be based. Also shown is the temperature dependence of the zero field dielectric constant for bulk $Sr_{0.5}Ba_{0.5}TiO_3$ which has been reduced 10 times to allow plotting on the same scale. On the right ordinate is plotted the percent change in the dielectric constant for a 200 kV/cm (10 V) applied bias field.

For integration into multilayer devices the surface morphology of the $Sr_xBa_{1-x}TiO_3$ thin films is important as well. In Fig 5 we show an SEM micrograph of a $Sr_{0.5}Ba_{0.5}TiO_3$ thin film, a $YBa_2Cu_3O_7$ thin film, and a $Sr_{0.8}Ba_{0.2}TiO_3$ thin film at the same magnification. These two $Sr_xBa_{1-x}TiO_3$ stoichiometries shown in Fig. 5 will likely be used in microwave devices operating at room temperature and 77K (with HTS metallization), respectively. The $YBa_2Cu_3O_7$ thin film, which was deposited under the same conditions as the $Sr_xBa_{1-x}TiO_3$ films and was not optimized for surface morphology, is shown for comparison. Fig. 5 shows the extremely smooth surface morphologies of $Sr_xBa_{1-x}TiO_3$ thin films deposited by pulsed laser deposition. In fact, these are among the

smoothest of all the materials our laboratory has deposited. In each case, the undesired presence of particulates is observed, but it is clear that thesed are minimized for the $Sr_xBa_{1-x}TiO_3$ thin films.

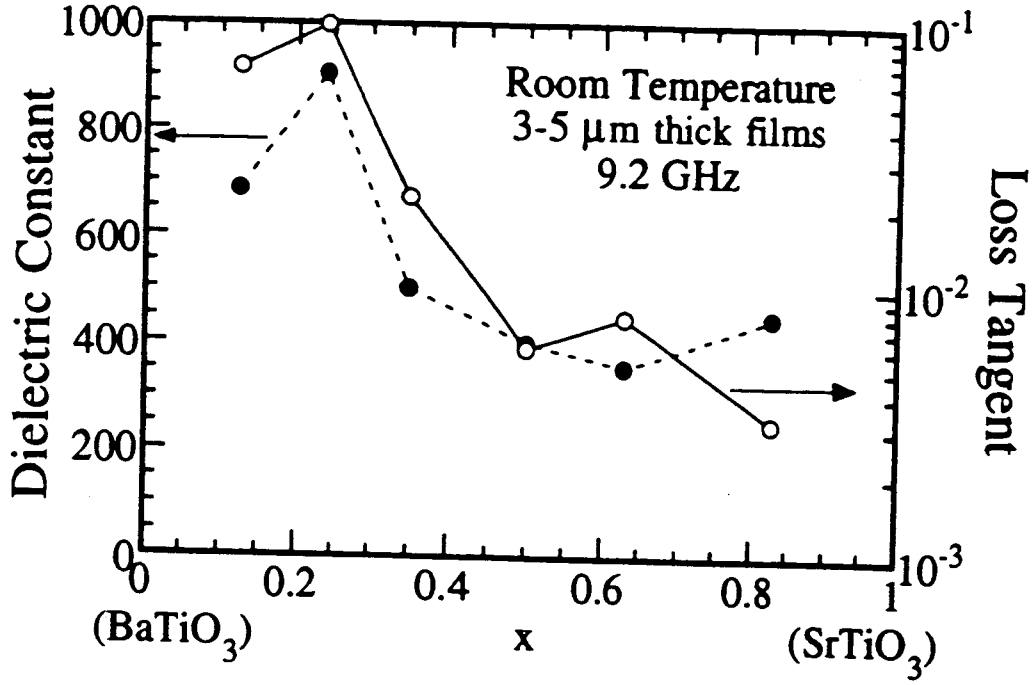

Figure 7. Variation of the dielectric constant and loss tangent with composition for $Sr_xBa_{1-x}TiO_3$ films deposited onto MgO and $LaAlO_3$ substrates. This measurement was done at room temperature at 9.2 GHz.

The electric field and temperature dependence of the dielectric constant for thin films of $Sr_{0.5}Ba_{0.5}TiO_3$ were measured by fabricating a simple microstrip transmission line. Using a $YBa_2Cu_3O_7/Sr_{0.5}Ba_{0.5}TiO_3$ bilayer on a (100) MgO substrate, a 1 µm thick Ag film was e-beam deposited and photolithographically patterned into 10.8 µm x 1 cm long transmission lines. The amplitude and phase of the transmitted signal (S_{21}) in the transmission line was measured as a function of the electric field for several temperatures at frequencies between 100 kHz and 0.1 GHz and the relative dielectric constant calculated. This data as well as the zero field data for bulk $Sr_{0.5}Ba_{0.5}TiO_3$, is shown in Fig. 6. The Curie temperature for this thin film can be determined from the peak in the zero field curve which occurs at ~220°C. Controlling the Curie temperature is important since it permits maximum tuning and device performance to be realized at or near the device operating temperature, e.g., room temperature or 77 K depending on the metallization layers. The Curie temperature for the film shown in Fig. 6 is different in two ways from that observed in the bulk. It is ~20-30°C lower in temperature and is much broader. Furthermore, the absolute value of the dielectric constant is about a factor of twenty less in the thin film that for the bulk. The proposed cause of this difference is strain in the film. For convenience,

Fig. 6 also shows on the right ordinate, the percent change in the dielectric constant as the bias voltage is changed between 0 and 10 volts. The maximum tunability occurs near the Curie temperature and it falls off much more rapidly above this temperature than below it.

An important requirement for the application of ferroelectrics in microwave devices is low dielectric loss. Dielectric loss degrades the Q and thus the electrical performance of a microwave device. Unusually high dielectric losses, as compared to the bulk, could preclude the use of $Sr_xBa_{1-x}TiO_3$ thin films in active microwave devices. In Fig. 7, we plot the dielectric constant and the dielectric loss tangent versus the Sr to Ba doping or x. This measurement was made on several different films of varying stoichiometry by the cavity perturbation technique described earlier. This figure shows the loss tangent is very sensitive to the Curie temperature of the deposited film, i.e., the loss tangent was greatest for films whose stoichiometry positioned the Curie temperature nearest to room temperature. As this is also the region of maximum tunability a balancing of these two issues must be made for the particular application of interest. Fig. 7 shows the dielectric loss of PLD-deposited $Sr_xBa_{1-x}TiO_3$ thin films to be as low as 0.1%. This is one of the lowest values ever measured for a ferroelectric thin film. The origin of this low loss is certainly dependent on the high crystalline quality of the PLD-deposited $Sr_xBa_{1-x}TiO_3$ thin films. The structural quality of a deposited film is reflected in the full width at half maximum of the x-ray rocking curves (see Fig. 4). Lastly, it is comforting that the dielectric constant value for the thin films from two different techniques are consistent to within 50%.

6. CONCLUSIONS

The results presented here are extremely encouraging for the successful production of active microwave devices based on ferroelectric thin films. Pulsed laser deposition has demonstrated itself as a suitable technique for the fabrication of precursor $Sr_xBa_{1-x}TiO_3$ thin films and multilayers for these devices. The films produced were single crystalline and of extremely high quality as evidenced by their narrow rocking curves widths. The surface morphologies of the deposited $Sr_xBa_{1-x}TiO_3$ thin films were very smooth permitting heteroepitaxial multilayer integration. Most importantly, the active dielectric property of ferroelectric thin films was greater than 50% near the Curie temperature while the dielectric loss tangent was as low as ~0.1%. The improved electrical performance (switching speed, size, and input power) which active microwave devices based on ferroelectric thin films offer in comparison to conventional devices will ensure their rapid incorporation in next generation systems.

7. REFERENCES

1. D.B. Chrisey and G.K. Hubler, Pulsed Laser Deposition of Thin Films, Wiley Interscience, New York, 1994.
2. H.S. Newman, D.B. Chrisey, J.S. Horwitz, B.D. Weaver, and M.E. Reeves, "Microwave devices using $YBa_2Cu_3O_7$ films made by pulsed laser deposition", IEEE Trans. on Mag., 27(2), 2540-2543, 1991.
3. J.M. Pond, K.R. Carroll, J.S. Horwitz, and D.B. Chrisey, "$YBa_2Cu_3O_7/LaAlO_3/YBa_2Cu_3O_7$ trilayer transmission lines for measuring the superconducting penetration depth", IEEE Trans. on Appl. Supercond., 3(1), 1438-1441, (1993).
4. D.B. Chrisey, J.S. Horwitz, J.M. Pond, K.R. Carroll, P. Lubitz, K.S. Grabowski, R.E. Leuchtner, C.A. Carosella, and C.V. Vittoria, "Pulsed laser

deposition of novel HTS multilayers for passive and active device applications", IEEE Trans. on Appl. Supercond., 3(1), 1528-1531, (1993).

5. V.K. Varadan, D.K. Gohdgaonkar, V.V. Varadan, J.F. Kelly and P. Glikerdas, "Ceramic phase shifter for electronically steerable antenna systems", Microwave J., Jan., 116-120, (1992).

6. J.S. Horwitz, D.B. Chrisey, J.M. Pond, R.C.Y. Auyeung, C.M. Cotell, K.S. Grabowski, P.C. Dorsey, and M.S. Kluskens, "$Sr_xBa_{1-x}TiO_3$ thin films for active microwave device applications", J. Integr. Ferro., in press (1995).

7. S.B. Quadri, J.S. Horwitz, D.B. Chrisey, R.C.Y. Auyeung, and K.S. Grabowski, "X-ray characterization of extremely high quality $Sr_xBa_{1-x}TiO_3$ films grown by pulsed laser deposition" Appl. Phys. Lett., in press (1995).